Characteristic times of oxygen mass transfer at the liquid metal–vapour interface

E. RICCI
Istituto di Chimica Fisica Applicata dei Materiali del CNR, via De Marini 6, 16149 Genova, Italy

L. NANNI, E. ARATO, P. COSTA
Istituto di Ingegneria Chimica e di Processo "G.B. Bonino", Università di Genova, via dell'Opera Pia 15, 16145 Genova, Italy

The interactions of liquid metals and alloys with the environment mostly depends on the thermodynamic properties of the liquid surface. In fact, the surface tension is strongly influenced by the presence in the surrounding atmosphere of reactive gases through solution, adsorption mechanisms and/or surface reactions. In particular, oxygen, which shows a high surface activity towards a large number of metallic systems, is the most important contaminant of liquid metals and alloys.

Theoretical approaches for estimating the oxygen mass transfer at the liquid–vapour interface under inert atmosphere and vacuum have been developed already in order to relate the observed physical properties to the real surface composition data.

In the present work a model of the interfacial transport of a liquid metal–oxygen system under Knudsen conditions that foresees the temporal evolution of the interfacial composition is presented. The diffusion characteristic times for reaching steady-state conditions are evaluated in order to define two system "sizes" depending on the different oxygen transport mechanisms in the liquid phase.

An experimental study of the interface evolution is at present under way and preliminary results show a satisfactory agreement with theoretical studies.

Nomenclature

c = molar concentration (mol m^{-3})
D_O = diffusion coefficient of atomic oxygen in the metal (m^2 s^{-1})
f = function defined in Equation 41
k = partial transport coefficient for the mass transfer (mol s g^{-1} m^{-1})
K = transport coefficient (m s^{-1})
$\bar{M}$ = molecular weight (g mol^{-1})
N = molar flux between the gas and the condensed phase (mol m^{-2} s^{-1})
P_j = partial pressure of the j^{th} oxide (Pa)
P_M = vapour pressure of the pure metal (Pa)
P_{O_2} = partial pressure of molecular oxygen (Pa)
P_{tot} = total pressure (Pa)
r = radial co-ordinate (m)
R = drop radius (m)
$\mathscr{R}$ = gas constant (J mol^{-1} K^{-1})
s = liquid saturation degree
T = temperature of the system (K)
T_b = boiling temperature (K)
T_m = melting temperature (K)
T_w = temperature of the container wall (K)
t = time (s)
x_O = molar fraction of atomic oxygen in the liquid phase
y = molar fraction in the gas phase
α = condensation coefficient
Γ = Gibbs adsorption (mol m^{-2})
ν = stoichiometric coefficient

Subscript and superscript

b = bulk
D = diffusion
l = liquid
g = gas
O_2 = molecular oxygen
M = metal
j = j^{th} oxide
I = interface
0 = initial state
s = saturation state
st = steady state

1. Introduction

The studies on the interplay of all possible mechanisms of mass transport at the interface of liquid metal–gas systems are of a topical interest, from a scientific and a technological point of view. In particular, for the high temperature processes, the definition of

0022–2461

the factors controlling oxygen mass transport through the liquid metal interface as a function of the boundary conditions assume an important role also in the definition of the efficiency of technological processes. In fact, oxygen shows a strong surface activity towards a large number of metallic systems [1], and its presence, in practice, can never be avoided. For this reason, investigations on high-temperature capillarity are basic to evaluate the tensio-active effects of oxygen on the liquid metal surfaces through surface tension and contact angle measurements.

Because the high temperature capillarity processes are generally performed under controlled atmosphere or under a vacuum, it seems extremely useful to provide theoretical models, in addition to the experimental observations, which enable an accurate estimation to be made of both the degree of contamination of the surface, and the mechanism of the oxygen mass transfer at the liquid–gas interface, in order to relate the observed physical properties to the real surface composition data.

To attempt this goal, we have previously developed two theoretical descriptions [2, 3], on the basis of kinetic and transport theories, relating the mass exchange between liquid metals and the surrounding atmosphere at different oxygen partial pressures: the first one under inert atmosphere (He fluxing with an inlet pressure of $\approx 10^5$ Pa); the second one under a vacuum (total pressure lower than 1 Pa in the Knudsen regime).

In the first model, where diffusion is the main mass-transport mechanism in the gas phase, reactions between metal vapours and molecular oxygen are allowed to occur, establishing specific reaction regimes in which the oxygen can or cannot contaminate the liquid metal surface.

In the second one, a total pressure less than 1 Pa is considered, assuring the Hertz–Knudsen conditions of thermomolecular regime for the mass transport phenomena in the gas phase. In fact, under a vacuum, transport processes in the gas phase have no control over the total interphase mass exchange, because of the large mean free path of the molecules.

Moreover, when dealing with metals which form volatile oxides, condensation of the oxide vapours on the reactor walls must be taken into account; the removal of oxide vapours from above the metal surface can significantly displace the oxidation equilibrium, enhancing the rate of oxide vaporization; this effect can be exploited in some cases to deoxidize and/or purify the liquid metal.

Owing to the double contribution of molecular oxygen and volatile oxides to the oxygen flux to and from the surface, steady-state conditions can be established, in which no variations of composition of the two phases occur over time. The problem can be approached by evaluating the total oxygen and metal evaporation rates as functions of the overall thermodynamic driving forces.

Curves separating different "oxidation regimes", were drawn, which represent an accurate control tool of the oxygen contamination degree of liquid metals under a vacuum; they are useful in capillarity measurements, in order to relate the observed surface properties to the actual liquid composition.

In this paper we present a theoretical model, based on the assumption of the model described above and upgraded, concerning the oxygen transfer through the liquid–vapour interface under Hertz–Knudsen conditions, allowing the temporal evolution of the interfacial composition to be considered. The model allows the diffusion characteristic times for reaching steady-state conditions to be evaluated.

2. The model

Let us consider a liquid metal drop placed at the centre of a close chamber as an exemplification of the real experimental set-up. The following conditions apply:

1. The temperature near the drop is maintained at a uniform and constant value T, which is higher than that on the chamber walls, T_w.
2. Total pressure $P_{tot} < 1$ Pa is maintained inside the chamber: thus, Hertz–Knudsen conditions are assured for the mass transport in the gas phase [4].
3. The activity coefficient of the liquid metal is assumed to be unity.
4. Small amounts of dissolved oxygen are assumed not to affect significantly the vapour pressure of the pure metal, P_M, which is assumed to depend only on the temperature T.
5. The partial pressure of oxygen in the residual atmosphere, $P_{O_2,g}$ is considered to be constant.
6. A molar fraction $x_O \leq x_{O,s}$ of atomic oxygen is dissolved into the metal, where $x_{O,s}$ indicates the limit of solubility [5]. Above this limit, the formation reaction of the first stable oxide in the condensed phase: $M^{(cond)} + \nu O_2^{(gas)} = MO_{2\nu}^{(cond)}$, is shifted to the right.

The term "first oxide" denotes the oxide with the minimum oxygen content which is thermodynamically stable under the imposed conditions.

When $x_O = x_{O,s}$, that is when the metal and the oxide exist at the same time as different condensed phases, the atmospheric composition is fixed at constant T for a system at equilibrium, and it can be calculated from thermodynamic data. In particular, the vapour pressures $P_{j,s}$ of the species containing oxygen (suboxides) resulting from thermal decomposition of the oxide depend exclusively on T [3].

The oxygen diffusion inside the liquid metal drop and the interfacial interactions can be evaluated assuming the liquid metal drop as a rigid sphere. Under this assumption and under the conditions described above, the local oxygen mass balance in the drop can be expressed in spherical co-ordinates as

$$\frac{\partial x_O}{\partial t} = D_O \frac{1}{r^2} \frac{\partial}{\partial r}\left(r^2 \frac{\partial x_O}{\partial r}\right) \qquad 0 \leq r < R(t) \leq R_0 \tag{1}$$

where r is the radial co-ordinate which is zero at the centre of the drop, D_O is the diffusion coefficient of atomic oxygen in the metal, $R(t)$ and R_0 are the sphere

radius at time t and at initial time $t = 0$, respectively. The possibility of a drop shrinking, due to the metal evaporation, is explicitly taken into account.

As initial conditions ($t = 0$ and $R = R_0$), we assume a uniform distribution of oxygen inside the drop

$$x_O = x_O^0 \qquad \text{for } 0 \le r < R \tag{2}$$

The assumed boundary conditions are: the symmetry condition at the drop centre

$$t > 0 \quad r = 0 \qquad \frac{\partial x_O}{\partial r} = 0 \tag{3}$$

the oxygen balance at the moving interface

$$t > 0 \quad r = R(t)$$

$$-c_l D_O \frac{\partial x_O}{\partial r} - 2N_{O_2,I} = (c_l x_{O,I} - c_g 2y_{O_2,I}) \frac{dR}{dt} \tag{4}$$

In Equation 4, c_l and c_g are the molar concentrations of the liquid and of the gas, respectively, $N_{O_2,I}$ is the flux of molecular oxygen at the interface, $y_{O_2,I}$ and $x_{O,I}$ are the molar fractions of molecular oxygen in the gas and of atomic oxygen in the metal respectively, near the interface. Equation 4 shows the oxygen flux arriving from the bulk to the interface ($-c_l D_O(\partial x_O/\partial r)$) and the oxygen flux going through the interface towards the gas phase ($N_{O_2,I}$), to be equal to the oxygen accumulation at the moving boundary.

The variation with time of the surface adsorption ($d\Gamma/dt$) is not considered in Equation 4; in fact, with reference to the known values of Γ for oxygen in liquid metals [1] and to the drop dimension considered ($R = 5 \times 10^{-3}$ m), the ratio between the oxygen mole number in the liquid bulk and those at the interface results much greater than one: i.e. $(Rc_l x_O/3\Gamma) \gg 1$ (for instance of the order of 10^3).

In addition to the boundary conditions, the total mass balance of the system has to be considered in order to deduce the interface evolution as a function of the net evaporation fluxes, both the oxygen flux at the interface $N_{O_2,I}$ and the metal flux $N_{M,I}$ coming from the interface

$$-(2N_{O_2,I} + N_{M,I}) = [c_l - c_g(2y_{O_2,I} + y_{M,I})] \frac{dR}{dt} \tag{5}$$

where $y_{M,I}$ is the molar fraction of the metal in the gas phase at the interface.

Because the concentration (density) of the gaseous phase is negligible compared with that of the liquid phase (i.e. $c_g \ll c_l$), the total mass balance (Equation 5), can be written in a more simple form, deducing the interface evolution which is directly dependent on the net evaporation fluxes

$$\frac{dR}{dt} = -\frac{2N_{O_2,I} + N_{M,I}}{c_l} \tag{6}$$

Substituting the total mass balance (Equation 6) in the expression of the total oxygen balance (Equation 4), the gradient of x_O at the interface can be defined

$$\left.\frac{\partial x_O}{\partial r}\right|_I = -\left[-2N_{O_2,I} + \left(x_{O,I} - \frac{c_g}{c_l} 2y_{O_2,I}\right) \times (2N_{O_2,I} + N_{M,I})\right](D_O c_l)^{-1} \tag{7}$$

As Equation 7 shows, the gradient of oxygen molar fraction depends on the oxygen flux at the gas–liquid interface, on the concentration discontinuity between the interfacial gas and the interfacial liquid and on the interface displacement which is correlated to the oxygen and metal fluxes.

If the condition $c_g 2y_{O_2,I} \ll c_l x_{O,I}$ is assumed, which is a more restrictive condition than $c_g \ll c_l$ but generally verified because of the rarefaction of the gas at the total pressure considered by the initial condition, the expression of the gradient of oxygen molar fraction at the interface (Equation 7) yields

$$\left.\frac{\partial x_O}{\partial r}\right|_I = -[(1 - x_{O,I}) 2N_{O_2,I} - x_{O,I} N_{M,I}](D_O c_l)^{-1} \tag{8}$$

As a further approximation, when $x_{O,I} \ll 1$ is assumed, which is reasonable in many cases, the gradient at the interface simply becomes

$$\left.\frac{\partial x_O}{\partial r}\right|_I = -\frac{2N_{O_2,I}}{D_O c_l} \tag{9}$$

Under this approximation, the oxygen concentration gradient at the interface depends on the evaporation flux and on the oxygen diffusivity ratio, but is independent of the evolution of the interface.

Taking into account Equation 9, the oxygen balance expressed by Equation 4 becomes

$$(c_l x_{O,I} - c_g 2y_{O_2,I}) \frac{dR}{dt} = 0$$

which, on the basis of the assumption made above, can be interpreted also as

$$\frac{dR}{dt} \approx 0 \tag{10}$$

which confirms that the variation in size of the drop is negligible.

3. Evaluation of steady-state conditions

The steady-state conditions of the system corresponds to a uniform and constant drop composition

$$x_O = x_{O,I} \quad \text{and} \quad \frac{\partial x_O}{\partial t} = 0 \qquad \text{for } 0 \le r < R \tag{11}$$

In particular, the liquid–vapour interface is considered to be in steady state when the oxygen concentration gradient in the liquid phase is zero, i.e.

$$\left.\frac{\partial x_O}{\partial r}\right|_I = 0 \tag{12}$$

As the condition to reach the steady state at the liquid–vapour interface (Equation 12) is implicit in the

condition of the steady-state of the system (Equation 11), it can be stated that the steady-state of liquid–vapour interface is a necessary condition to reach the steady state of the drop. Obviously, such a condition can be verified when all fluxes at the liquid–vapour interface are zero

$$N_{O_2,I} = N_{M,I} = 0 \tag{13}$$

Equation 13 defines the thermodynamic equilibrium at the liquid–vapour interface which is consistent with a null gradient and a steady interface, and results in the kinematics steady-state condition $dR/dt = 0$. However, the steady state at the interface can also be achieved under less restrictive conditions than that imposed by Equation 13; in fact Equation 12 is verified (see Equation 8) also when a sort of flux congruence is achieved

$$\frac{2N_{O_2,I}}{N_{M,I}} = \frac{x_{O,I}}{1 - x_{O,I}} \tag{14}$$

In fact, the presence of non-zero fluxes does not necessarily modify the composition of the liquid phase; on the other hand, when a net flux of matter crosses the liquid–vapour interface, under the steady condition (Equation 14), a time variation of the drop dimensions occurs

$$\frac{dR}{dt} = -\frac{2N_{O_2,I}}{x_{O,I}c_l} \tag{15}$$

Moreover, under the frequently verified condition for which the oxygen flux at the interface is less than the metal evaporation flux

$$2N_{O_2,I} \ll N_{M,I} \tag{16}$$

Equation 14 can be simplified to

$$N_{O_2,I} = 0 \quad \text{and} \quad N_{M,I} \neq 0 \tag{17}$$

This approximation is consistent with Equations 9 and 10. In this case the velocity of the interface can be evaluated from Equation 15 while the study of transitions to the steady-state condition can be carried out under the approximation of constant dimensions as expressed by Equation 10.

In the following, we refer to this latter approach, which seems to be sufficient to approximate the experimental conditions in the short times.

4. Characteristic times

In order to examine the physical meaning of the steady-state condition and to evaluate the time necessary to reach it, some characteristic times have to be evaluated. The diffusion time within the drop is defined [6] as

$$t_D = \frac{R^2}{9D_O} \tag{18}$$

The time t_{st} necessary for a homogenous drop to reach the steady-state composition x_O^{st} can be estimated first by a space integration of Equation 1 together with Equations 2, 3 and 9, obtaining

$$\frac{d\bar{x}_O}{dt} = -\frac{6N_{O_2,I}}{Rc_l} \tag{19}$$

Then, with reference to the mean value of the flux

$$\bar{N}_{O_2,I} = \frac{(N^0_{O_2,I} + N^{st}_{O_2,I})}{2} \approx \frac{N^0_{O_2,I}}{2} \tag{20}$$

(where $N^0_{O_2,I}$ and $N^{st}_{O_2,I}$, are the interface oxygen fluxes at the initial state and at the steady state, respectively), and to the initial ($\bar{x}_O = x_O^0$) and final ($\bar{x}_O = x_O^{st}$) composition, the approximate time integration of Equation 19 allows the characteristic time to be evaluated

$$t_{st} = \frac{1}{3}\frac{Rc_l}{N^0_{O_2,I}}(x_O^0 - x_O^{st}) \tag{21}$$

By comparing the characteristic times t_D, as defined in Equation 18, and t_{st}, two subclasses of systems can be distinguished: "small" and "large" drops, depending on the different mechanism of the oxygen transport in the liquid phase.

4.1. "Small" drops

We define the drop as "small", when the diffusion time within the drop is very small (related to the system parameters), so that the drop composition can be taken as uniform ($x_O = x_{O,I}$; $0 \leq r < R$; $t > 0$) and the condition $t_D \ll t_{st}$ is verified. From a geometrical point of view, taking into account Equations 18 and 21, this condition is equivalent to

$$R \ll \frac{3D_O c_l}{N^0_{O_2,I}}(x_O^0 - x_O^{st}) \tag{22}$$

As the "small" drop, defined in Equation 22, shows uniform composition, the characteristic time of the bulk, t_b, and that of the interface, t_I, are equal to t_{st}, then

$$t_I = t_b = t_{st} \gg t_D$$

Thus, for "small" drops, the characteristic time is calculated according to Equation 21 and the steady-state condition $x_O = x_{O,I} = x_O^{st} = \text{const}$, is achieved at the same time both at the interface and in the bulk.

4.2. "Large" drops

We define the drop as "large" when $t_D \gg t_{st}$ and Equation 22 becomes

$$R \gg \frac{3D_O c_l}{N^0_{O_2,I}}(x_O^0 - x_O^{st}) \tag{22a}$$

In this case the diffusion within the liquid metal drop is the controlling process.

The time t_b is of the same order of t_D, while t_I should be much shorter and could be evaluated equalling the diffusional penetration distances.

The same result can be obtained by following a formal approach, allowing the interfacial composition to

be calculated from the convolution integral

$$x_{O,I} = x_O^0 - \frac{1}{c_l(\pi D_O)^{1/2}} \int_0^t \frac{2N_{O_2,I}[x_{O,I}(t')]}{(t-t')^{1/2}}\,dt' \quad (23)$$

Equation 23 is correct for planar geometry, but it is fully acceptable also for spherical geometry if the diffusion penetration distance is much smaller than the drop radius.

Substituting the mean value of flux (Equation 20) in Equation 23, an estimation of the characteristic time of the interface t_I, is obtained

$$t_I = \pi \frac{D_O c_l^2 (x_O^0 - x_O^{st})^2}{(2N_{O_2,I}^0)^2} \quad (24)$$

A correlation between the characteristic times can be obtained by using Equations 18 and 21 and assuming the approximation: $\pi^{1/2} \approx 2$

$$t_I = \frac{t_{st}^2}{t_D} \quad (25)$$

So, for "large" drops: $t_I = t_{st}^2/t_D \ll t_{st} \ll t_b \approx t_D$. In this case the interface reaches the steady-state composition in a characteristic time t_I defined by Equation 24 or 25, which is much less than t_b. This last time is also much longer than the time t_{st} associated with a homogeneous drop, and it is practically controlled by the diffusion time t_D.

5. Temporal evolution of the interface

The trend of the oxygen interfacial composition versus time, the initial conditions defined in Equation 2 being valid, can be described by the differential Equation 19 for "small" drops, and by the integral Equation 23 for "large" drops. The inequalities (Equations 22 and 22a) discriminate between "small" and "large" drops.

In particular, as a simple case, the example of an overall oxygen flux linearly dependent on the driving force is reported. By assuming for the overall atomic oxygen flux

$$2N_{O_2,I} = Kc_l(x_{O,I} - x_O^{st}) \quad (26)$$

(where K is the transport coefficient for the oxygen), the characteristic times of the interface for the two subclasses considered, on the basis of Equations 21 and 24 are, respectively

$$t_I = \frac{2}{3}\frac{R}{K} \qquad \text{for "small" drops} \quad (27)$$

and

$$t_I = \frac{4D_O}{K^2} \qquad \text{for "large" drops} \quad (28)$$

For "small" drops, the analytical solution of Equation 19 yields an exponential dependence on time of the oxygen interface composition in the liquid phase

$$\frac{x_{O,I} - x_O^{st}}{x_O^0 - x_O^{st}} = e^{-2t/t_I} \quad (29)$$

On the other hand, for "large" drops, also Equation 23 admits the analytical solution

$$\frac{x_{O,I} - x_O^{st}}{x_O^0 - x_O^{st}} = e^{4t/t_I}\,\mathrm{erfc}(4t/t_I)^{1/2} \quad (30)$$

In particular, for $t \gg t_I$ Equation 30 degenerates to

$$\frac{x_{O,I} - x_O^{st}}{x_O^0 - x_O^{st}} \approx \left(\frac{t_I}{4\pi t}\right)^{1/2} \approx \frac{1}{K}\left(\frac{D_O}{\pi t}\right)^{1/2} \quad (31)$$

which is an expression of an approximate trend of the dependence on time of the oxygen interface composition in the liquid phase for "large" drops. In this case also, the expression of the flux at the interface degenerates in the well known trend at constant composition $x_{O,I}$

$$2N_{O_2,I} \approx (x_O^0 - x_O^{st})\left(\frac{D_O}{\pi t}\right)^{1/2} \quad (32)$$

However, in more general cases, where the interfacial flux $N_{O_2,I}$ is non-linear, the characteristic times also depend on the concentrations.

As already described in the previous model [3], concerning the oxygen mass transfer at liquid–metal-vapour interface under a low total pressure, with its assumptions remaining valid, the total oxygen and metal fluxes at the interface are written as

$$N_{O_2,I} = k_{O_2}(s_I^2 P_{O_2,s} - P_{O_2,g}) + \Sigma_j \nu_j k_j (s_I^{2\nu_j} P_{j,s} - P_{j,g}) \quad (33)$$

$$N_{M,I} = k_M(P_{M,s} - P_{M,g}) + \Sigma_j k_j (s_I^{2\nu_j} P_{j,s} - P_{j,g}) \quad (34)$$

where k_{O_2}, k_M, and k_j, are the coefficients of the Hertz–Langmuir–Knudsen [4] equation for the evaporation from a surface under a vacuum. For an evaporating element or a compound, such a coefficient is given by

$$k = \alpha\left(\frac{1}{2\pi \mathscr{R} T \bar{M}}\right)^{1/2} \quad (35)$$

where α is the condensation coefficient of the evaporating species and $\bar{M}$ is the molecular weight.

Equations 33 and 34 describe the system in terms of coefficients and driving forces related to the gaseous phase only. In the expression of the driving forces appears the relative saturation of the interfacial liquid.

The steady-state condition for the interface (Equation 14 or 17) combined with Equations 33 and 34 leads to individuate the value of the steady-state liquid saturation degree s_{st}, as a function of the gaseous phase composition ($P_{O_2,g}$, $P_{j,g}$, $P_{M,g}$), of the values at saturation ($P_{O_2,s}$, $P_{j,s}$, $P_{M,s}$) and of the liquid phase ($x_{O,s}$), which in turn depend on temperature. In the expression of s_{st} also the transport coefficient ratio

$$\phi_j = \frac{k_j}{k_{O_2}} = \frac{\alpha_j}{\alpha_{O_2}} \frac{1}{(m+\nu_j)^{1/2}} \quad (36)$$

appears, where m is the molecular weight ratio $= \bar{M}_M/\bar{M}_{O_2}$. By taking into account Equations 17, 33 and 36, the "steady-state saturation degree" $s_{st} = x_O^{st}/x_{O,s}$ can be derived by the following equation, which is

solvable by an iterative procedure

$$s_{st} = \left[\frac{P_{O_2,g} + \Sigma_j \nu_j \phi_j P_{j,g}}{P_{O_2,s} + \Sigma_j \nu_j \phi_j P_{j,s} s_{st}^{2(\nu_j - 1)}} \right]^{1/2} \quad (37)$$

As expected, when the saturation values of oxygen pressure, $P_{O_2,g} = P_{O_2,s}(T)$ and the vapour pressure of species containing oxygen, $P_{j,g} = P_{j,s}(T)$ are imposed (oxygen saturation, with the system in monovariant equilibrium), s_{st} becomes equal to unity.

When, as in this case, the steady-state condition can be approximated with Equation 17 ($N^{st}_{O_2,I} = 0$), the oxygen flux at the interface (Equation 33) in the steady state can be written in the form

$$N^{st}_{O_2,I} = k_{O_2,I} P_{O_2,s} (s_I^2 - s_{st}^2) + \Sigma_j \nu_j k_{j,I} P_{j,s} (s_I^{2\nu_j} - s_{st}^{2\nu_j}) \quad (38)$$

and, by the same way, the initial flux $N^0_{O_2,I}$, which is non-linear with respect to the term $(s_0^2 - s_{st}^2)$, results

$$N^0_{O_2,I} = k_{O_2,I} P_{O_2,s} (s_0^2 - s_{st}^2) + \Sigma_j \nu_j k_{j,I} P_{j,s} (s_0^{2\nu_j} - s_{st}^{2\nu_j}) \quad (39)$$

Then, the characteristic time t_{st}, as defined in Equation 21, depends on the initial composition of the liquid and, on the basis of Equation 39, it can be written as

$$t_{st} = \frac{R c_1 x_{O,s}}{3 k_{O_2} P_{O_2,s}} \frac{1}{f(s_0, s_{st})} \quad (40)$$

where f is

$$f = \left[s_0^2 - s_{st}^2 + \Sigma_j \nu_j \phi_j \frac{P_{j,s}}{P_{O_2,s}} (s_0^{2\nu_j} - s_{st}^{2\nu_j}) \right] (s_0 - s_{st})^{-1} \quad (41)$$

6. Applications

For the sake of simplicity, the factor f can be approximated under different conditions as follows:

(1) if $s_0 \gg s_{st}$

$$f \approx s_0 \left[1 + \Sigma_j \nu_j \phi_j \frac{P_{j,s}}{P_{O_2,s}} s_0^{2(\nu_j - 1)} \right] \quad (42)$$

(2) if $s_0 \approx s_{st}$

$$f = 2 s_0 \left[1 + \Sigma_j \nu_j^2 \phi_j \frac{P_{j,s}}{P_{O_2,s}} s_0^{2(\nu_j - 1)} \right] \quad (43)$$

In particular, Equation 42 can be usefully applied to calculate t_{st} when the initial condition of the system is the saturation ($s_0 = 1$). In this case, the condition $s_0 \gg s_{st}$ is largely verified and the factor f can be further approximated in

$$f \approx 1 + \Sigma_j \nu_j \phi_j \frac{P_{j,s}}{P_{O_2,s}} \quad (44)$$

Under these conditions the characteristic time t_{st} can be calculated by the relationship obtained from Equations 40 and 44

$$t_{st} = \left(\frac{R c_1 x_{O,s}}{3 k_{O_2} P_{O_2,s}} \right) \left[1 + \Sigma_j \nu_j \phi_j \left(\frac{P_{j,s}}{P_{O_2,s}} \right) \right]^{-1} \quad (45)$$

The characteristic time t_{st} for some metallic systems of technological interest has been calculated by using Equation 45, considering, as a first approximation, the ratio of the condensation coefficients α_j and α_{O_2} to be equal to unity if the efficiency of the evaporating process is assumed to have about the same value for both species.

The thermodynamic quantities have been calculated as a function of temperature starting from the melting temperature up to the boiling temperature at the fixed total pressure of 10^{-3} Pa. The partial pressures $P_{O_2,s}$ and $P_{j,s}$ have been calculated by evaluating the equilibrium constants of the reaction of formation of the first stable oxide and the volatile oxides, respectively [7], on the basis of equilibrium constant of the oxidation reaction.

The value of the characteristic time t_{st} was then calculated for each metal as a function of temperature. As an example, the values referred to the liquid tin are reported in Table I.

The values of t_{st} as a function of temperature at a total pressure $P_{tot} = 10^{-1}$ Pa for a set of selected

TABLE I Characteristic time t_{st} as a function of temperature of a liquid tin drop ($R = 5 \times 10^{-3}$ m) from melting to boiling point at a total pressure $P_{tot} = 10^{-3}$ Pa and related thermodynamic quantities

Temperature (K)	Density (kg m^{-3})	$x_{O,s}$	$P_{j,s}$ (Pa)	$P_{j,s}$ (Pa)	$P_{O_2,s}$ (Pa)	t_{st} (s)
			j = SnO	j = SnO_2		
506	6999.5	7.20E−10	1.20E−18	3.90E−25	4.30E−45	6.96E + 12
556	6966.3	7.70E−09	8.30E−16	3.60E−20	1.20E−39	1.14E + 11
606	6933.4	5.60E−08	1.90E−13	5.00E−16	4.20E−35	3.70E + 09
656	6900.8	3.00E−07	1.90E−11	1.60E−12	2.90E−31	1.79E + 08
706	6868.5	1.30E−06	9.90E−10	1.60E−09	5.90E−28	4.28E + 06
756	6836.5	4.50E−06	3.00E−08	6.60E−07	4.30E−25	4.93E + 04
806	6804.8	1.30E−05	5.90E−07	1.30E−04	1.40E−22	8.16E + 02
856	6773.4	3.50E−05	8.20E−06	1.30E−02	2.20E−20	2.16E + 01
906	6742.2	8.40E−05	8.40E−05	7.80E−01	2.00E−18	8.59E−01
956	6711.4	1.80E−04	6.80E−04	3.10E+01	1.10E−16	4.82E−02
1006	6680.8	3.70E−04	4.40E−03	8.40E+02	4.40E−15	3.62E−03
1056	6650.6	6.90E−04	2.40E−02	1.70E+04	1.20E−13	3.49E−04
1106	6620.6	1.20E−03	1.10E−01	2.50E+05	2.30E−12	4.19E−05
1156	6590.8	2.10E−03	4.40E−01	3.00E+06	3.50E−11	6.06E−06

Element: Sn.
Total pressure: 10^{-3} (Pa).
Melting point: 505 K. Boiling point: 1158 K.

TABLE II Values of t_{st}(s) as a function of temperature at a total pressure $P_{tot} = 10^{-1}$ Pa for a set of selected liquid metal drops ($R = 5 \times 10^{-3}$ m)

$P_{tot} = 10^{-1}$ Pa	Al $T_m = 933$ K	Ga $T_m = 303$ K	In $T_m = 430$ K	Ge $T_m = 1211$ K	Sn $T_m = 505$ K	Pb $T_m = 601$ K
T_m	8.91E+02	5.94E+13	8.75E+35	7.18E−03	6.96E+12	1.52E+09
$T_m + 100$ K	8.70E+01	4.16E+08	6.41E+27	2.28E−03	3.70E+09	8.21E+06
$T_m + 200$ K	1.32E+01	3.70E+05	1.90E+22	9.15E−04	4.28E+06	1.71E+03
$T_m + 500$ K	–	1.35E+01	8.05E+12	–	3.62E−03	–
$T_m + 600$ K	–	2.20E+00	1.03E+11	–	4.19E−05	–

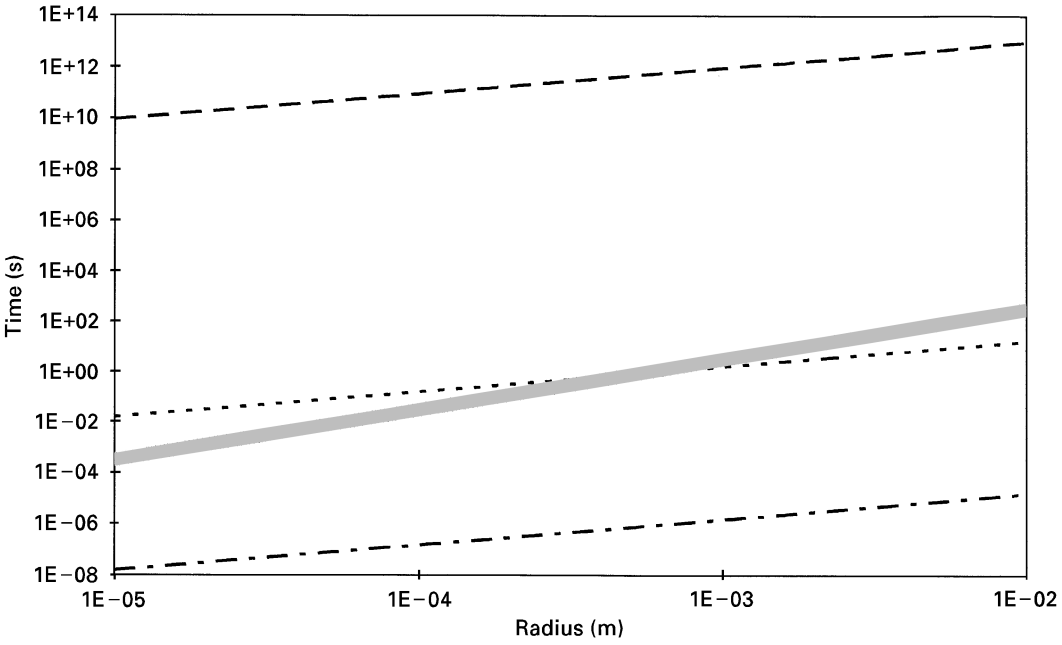

Figure 1 Isotherm trend of the characteristic time t_{st} of liquid tin as a function of the drop radius R at $P_{tot} = 10^{-3}$ Pa. (– –) characteristic time calculated at melting point (505 K); (— - —) characteristic time calculated at boiling point (1158 K); (- - -) characteristic time at an intermediate $T = 870$ K; Bold curve: diffusion times calculated for T from 1023 K to 1158 K and extrapolated for T from 505 K to 1023 K.

metals are reported in Table II. By comparing the reported values of t_{st} calculated under fixed conditions of temperature ($T_m < T < T_b$) and pressure for different liquid metal drops having constant dimensions, with the estimated [8–11] corresponding values of oxygen diffusion times in the liquid metal ($t_D = 10^1$–10^3 s), the two subclasses can be recognized; "small" drops when $t_{st} \gg t_D$ and "large" drops when $t_{st} \ll t_D$, as defined by the theoretical model. A tin drop, for example, can be considered "small" up to a temperature of about 700 K, but for temperatures above 1000 K it can be considered "large". Drops of In or Pb can be considered "small" in the overall range of temperature considered here. On the other hand, a drop of Ge can be considered always as "large".

As a clarifying example, Fig. 1 shows that the classification in "small" or "large" drops not only depends on the drop's radius but mostly on the liquid metal temperature. The trend of t_{st} as a function of the radius of a liquid tin drop is shown at three fixed temperatures. The trend of t_D is also reported: diffusion times have been calculated at the boiling temperature on the basis of available literature data [9] and extrapolated for $T < 1023$ K. It can be noticed that despite a small radius, at a temperature near the boiling point, a liquid tin drop is classified as "large", whereas for a temperature near the melting one the drop is "small". For the intermediate temperatures some t_{st} curve may cross the corresponding t_D curve and a fixed radius can be singled out which discriminate the belonging to "small" or "large" drop class.

7. Conclusions

A theoretical model to evaluate the interfacial transport of a liquid metal–oxygen system under Knudsen conditions has been developed.

Starting from a local oxygen mass balance in the liquid metal drop and taking into account the total mass balance, the oxygen molar fraction at the interface and in the liquid phase have been evaluated as a function of time.

Steady-state conditions have been defined for this particular system both for the bulk liquid phase and the interface. The evaluation of the relevant characteristic times (for diffusion, and to reach stationary conditions) has allowed two characteristic system "sizes" to be defined: "small" and "large" drops, depending on the different mechanisms of gas transport in the liquid phase.

The interfacial characteristic times and the trend of the oxygen interfacial composition vs. time have been

calculated for "small" and "large" drops in some simple cases.

Finally, the present model has been used to make some estimate of the behaviour of selected metallic systems under different conditions.

An experimental programme is currently under way in our laboratory to validate this model; preliminary results confirm the reliability of the characteristic times to reach a surface steady-state composition estimated by the present work.

Acknowledgements

The authors wish to thank Dr A. Passerone (ICFAM-CNR Genova) for his contribution during many fruitful discussions on this subject.

References

1. C. H. P. LUPIS, in "Chemical thermodynamics of materials" (Elsevier Publishers, Amsterdam, Netherlands, 1983).
2. E. RICCI, A. PASSERONE, P. CASTELLO and P. COSTA, *J. Mater. Sci.* **29** (1994) 1833.
3. P. CASTELLO, E. RICCI, A. PASSERONE and P. COSTA, *ibid.* **29** (1994) 6104.
4. R. OHNO, in "Liquid metals – chemistry and physics", edited by S. Z. Beer (Marcel Dekker Inc., New York, 1972) Chapter 2.
5. S. OTSUKA and Z. KOZUKA, *Trans. Jpn. Inst. Met.* **22** (1981) 558.
6. G. ASTARITA, "Mass transfer with chemical reaction" (Elsevier, Amsterdam, 1967).
7. O. KNACKE, O. KUBASCHEWSKI and K. HESSELMANN, "Thermo-chemical properties of inorganic substances" 2nd edition (Springer Verlag, Verlag Stahleisen m.b. H Düsseldorf, 1991).
8. P. RAJENDERA, P. CHHABRA and K. ROY, *Z. Metallkde.* **79** (1988) 64.
9. T. A. RAMANARAYANAN and R. A. RAPP, *Met. Trans.* **3** (1972) 3239.
10. R. SZWARC, K. E. OBERG and A. RAPP, *High Temp. Sci.* **4** (1972) 347.
11. K. A. KLINEDINST, and D. A. STEVENSON, *J. Electrochem. Soc.* **120** (1973) 304.

Received 26 February
and accepted 5 August 1997